Compressive Sensing Reconstruction of Wideband Antenna Radiation Characteristics

Patrick Debroux* and Berenice Verdin

Abstract—Characterization measurements of wideband antennas can be a time intensive and an expensive process as many data points are required in both the angular and frequency dimensions. Parallel compressive sensing is proposed to reconstruct the radiation-frequency patterns (RFP) of antennas from a sparse and random set of measurements. The modeled RFP of the dual-ridge horn, bicone, and Vivaldi antennas are used to analyze the minimum number of measurements needed for reconstruction, the difference in uniform versus non-uniform reconstruction, and the sparsity transform function used in the compressive sensing algorithm. The effect of additive white Gaussian noise (AWGN) on the minimum number of data points required for reconstruction is also studied. In a noise-free environment, the RFP of the antennas were adequately reconstructed using as little as 33% of the original data points. It was found that the RFPs were adequately reconstructed with less data points when the discrete cosine transforms (DCT), rather than the discrete Fourier transforms (DFT) was used in the compressive sensing algorithm. The presence of noise increases the number of data points required to reconstruct an RFP to a specified error tolerance, but the antenna RFPs can be reconstructed to within 1% root-mean-square-error of the original with a signal to noise ratio as low as -15 dB. The use of compressive sensing can thus lead to a new measurement methodology whereby a small subset of the total angular and frequency measurements is taken at random, and a full reconstruction of radiation and frequency behavior of the antenna is achieved during post-processing.

1. INTRODUCTION

The measurement of wide-band antennas is often a long and expensive process requiring substantial anechoic chamber time to measure the radiated fields at all angles and all frequencies under consideration. A need has thus been identified for a method to adequately characterize the radiation pattern of wideband antennas using fewer measurement points.

Characterization data compactness has been achieved using model based parameter estimation (MBPE) that approximates the far-field radiation pattern using a simple antenna model and then augments and calibrates the model results using sparse measurements [1]. Research has been reported on using MBPE to interpolate the antenna's radiated fields in both the spatial and spectral domains so that changes in radiation pattern with frequency can be extrapolated [2]. The MBPE method is not completely empirical as the antenna must be modeled, albeit in rudimentary fashion, to properly interpolate the radiation patterns.

Reconstruction of antenna patterns from near-field measurements using the radiation centers of the antenna has been reported [3], while [4] reconstructed far-field radiation patterns from near-field amplitude measurements using the global particle swarm optimization (PSO). Rammal et al. [5] reconstructed wideband far-field radiation patterns from near-field transient measurements. Koh et

* Corresponding author: Patrick Debroux (patrick.s.debroux.civ@mail.mil).
The authors are with the Army Research Laboratory, Survivability and Lethality Analysis Directorate, White Sands Missile Range, New Mexico 88002-5513, USA.

al. [6] reconstruct antenna radiation patterns using impulse deconvolution to remove measurement clutter in non-anechoic chamber antenna characterization. These transform methods do not directly address pattern reconstruction from limited angular and frequency measurements.

Cost-effective compressive sensing reconstruction of a dense two-dimensional array from a sparse element array used for microwave imaging has been reported by [7]. Here, Wei et al. form the scattering matrix that include terms of each sparse array element and scatterer pair and transform it into the sparsity domain using a Fourier Transform. Compressive sensing is applied to reconstruct a dense scattering matrix inverted to image the scatterers. This application is intended to reconstruct dense microwave transmit antenna arrays from sparse ones when imagining scenes, but does not address the frequency behavior of wideband antennas.

In this study, Verdin and Debroux's [8] work on applying compressive sensing to the reconstruction of 2D far-field antenna patterns from randomly distributed measurements is extended to reconstruct 2D far-field wideband radiation patterns, in the form of radiation-frequency patterns (RFPs). We treat the antenna RFP as a sparse surface and reconstruct this surface using compressive sensing a single dimension at a time, using single dimensional data. This method leads to a new wideband antenna measurement method where the antenna is measured over a small percentage of randomly distributed angles and frequencies, and the far-field radiation pattern is reconstructed using parallel compressive sensing post-processing.

2. COMPRESSIVE SENSING

Compressive sensing has its roots in transform coding where a compressible signal is transformed to a domain where it is sparse (containing only a few large transform coefficients). The large coefficients mostly characterize the signal that can be adequately reconstructed by taking the inverse transform of only these large coefficients.

In transform coding, a data set, $\mathbf{x}$, can be represented [9] as

$$\mathbf{x} = \boldsymbol{\psi}\mathbf{s}, \tag{1}$$

where $\boldsymbol{\psi}$ is an $N \times N$ basis matrix, and $\mathbf{s}$ is an $N \times 1$ column vector of weighing coefficients. The data set $\mathbf{x}$ is said to be K-sparse if $\mathbf{s}$ contains only K coefficients in the transform domain. If $K < N$, the signal is said to be compressible.

Transform coding is useful for data storage but assumes that the signal is completely known before taking its transform. Compressive sensing begins with an under-sampled signal and attempts to reconstruct the signal using an inversion scheme and an optimization using the ℓ_1-norm [9].

If $\mathbf{y}_M$ measurements are taken of the data set $\mathbf{x}_N$, where $M < N$, the basis matrix $\boldsymbol{\psi}$ can be adjusted for the number of measurements taken by keeping the basis functions rows that correspond only to the measurements taken [10]. This can be written as

$$\mathbf{y} = \boldsymbol{\Theta}\mathbf{s} \tag{2}$$

where $\mathbf{y}$ is a vector of the M measurements, $\boldsymbol{\Theta} = \mathbf{R}\boldsymbol{\psi}$ is the $M \times N$ basis matrix ($\boldsymbol{\psi}$ modified by an operator $\mathbf{R}$ that keeps only the rows associated with the measurements taken), and $\mathbf{s}$ is the data set to be reconstructed in the sparse domain. Eq. (2) is now dimensionally suited to solve for $\mathbf{s}$ from a limited number, M $(< N)$, of measurements.

The locations of the large K-coefficients are not known *a-priori*, but the conditions sufficient for stable reconstruction can be achieved by using random rows of the basis function, $\boldsymbol{\psi}$ [11].

The key to the compressive sensing process is to find and use a transform that will render the signal sparse in the transform domain. Common transforms used in compressive sensing are the discrete Fourier transform (DFT) and the discrete cosine transform (DCT). Once a transform is chosen, it is cast in a discrete matrix form to allow solving for $\mathbf{s}$ in Eq. (2). For example, the DFT matrix, $\boldsymbol{\psi}_{N,N}$ can be written as

$$\boldsymbol{\psi}_{N,N} = \frac{1}{\sqrt{N}} \begin{bmatrix} e^{\frac{-j2\pi n_1 k_1}{N}} & \cdots & e^{\frac{-j2\pi n_1 k_N}{N}} \\ \vdots & \ddots & \vdots \\ e^{\frac{-j2\pi n_N k_1}{N}} & \cdots & e^{\frac{-j2\pi n_N k_N}{N}} \end{bmatrix}. \tag{3}$$

The $\boldsymbol{\Theta}_{M,N}$ matrix is then inverted and multiplied by the measurements to yield the reconstructed data in the sparse domain

$$\mathbf{s} = \boldsymbol{\Theta}^{-1}\mathbf{y}. \tag{4}$$

Since Eq. (2) is under-constrained, because $M < N$, an infinite amount of solutions, $\mathbf{s}'$, exist in the reconstruction of the total data set of length N from M measurements. The signal $\mathbf{s}$ is approximated by $\hat{\mathbf{s}}$ that is estimated using an iterative ℓ_1-norm minimization routine [9]. The reconstructed data set whose sum of its elements is minimum is chosen, so that

$$\mathbf{s} \simeq \hat{\mathbf{s}} = \arg\min \|\mathbf{s}'\|_{\ell_1}. \tag{5}$$

A signal of length N can be reconstructed with as little as M random measurement where $M \geq cK\log(N/K)$, K is the number of non-zero elements of the signal transformed in the sparsity domain, and c is a small constant [12]. In this work, the ℓ_1-magic collection of algorithms [13] was used to reconstruct the antenna RFPs from sparse and randomly distributed measurement points.

3. RADIATION-FREQUENCY PATTERN RECONSTRUCTION

Three antennas were modeled [14] to calculate radiation-frequency patterns (RFP) over a relatively wide band. The RFPs were reconstructed to analyze the success of the compressive sensing method for this application. The wideband antennas modeled were the dual-ridge horn, the bicone, and the Vivaldi antennas. RFPs were calculated in $1°$ increments in the antenna H-plane azimuth dimension, with 100 calculations equally spanning the specified bandwidth.

Because the reconstruction of the RFP is performed in both the angular and frequency dimensions, the radiation pattern is reconstructed one frequency at a time, meaning that each row of the angle-frequency calculation matrix is reconstructed individually. The resulting reconstruction is then transposed and the frequency behavior of the antenna is reconstructed one angle at a time. This concept of parallel compressed sensing was reported by [15]. The radiation and the frequency dimensions of the RFP can be reconstructed sequentially using the same random distribution of data points in each dimension (uniform reconstruction), or with different random distributions of data points (non-uniform reconstruction) in each dimension [10].

Reconstruction of the RFP of the three antenna models are performed using the DFT and the DCT, using uniform and non-uniform random frequency measurement distributions, and in the presence of noise. The results are analyzed to determine the minimum amount of calculated points needed for adequate reconstruction. In this research, the number of randomly distributed calculated points used to reconstruct the RFP is the same in both the angular and frequency dimensions.

3.1. Dual-ridge Horn Antenna Reconstruction

The total far-field electric field, E_{total} RFP of a dual-ridge (with aperture measuring $24.5\,\text{cm}$ by $14.5\,\text{cm}$) was modeled between the frequencies of $2\,\text{GHz}$ and $6\,\text{GHz}$, and is shown in Fig. 1. Superimposed on the RFP are the data points used to calculate the surface.
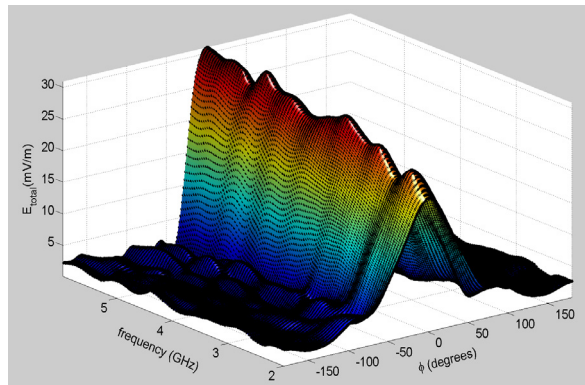

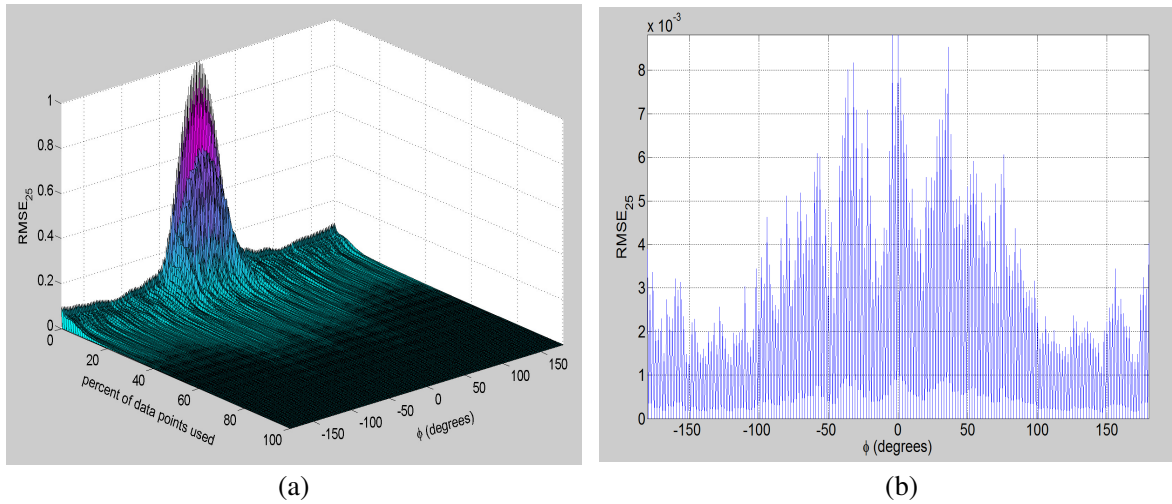**Figure 1.** The RFP of the dual-ridge horn antenna.

Figure 2. (a) The average RMSE of the normalized DCT reconstruction of the dual-ridge horn RFP as a function of the number of data points used. (b) The RMSE of a cross-cut of Fig. 2(a) taken when 33% of data is used for reconstruction.
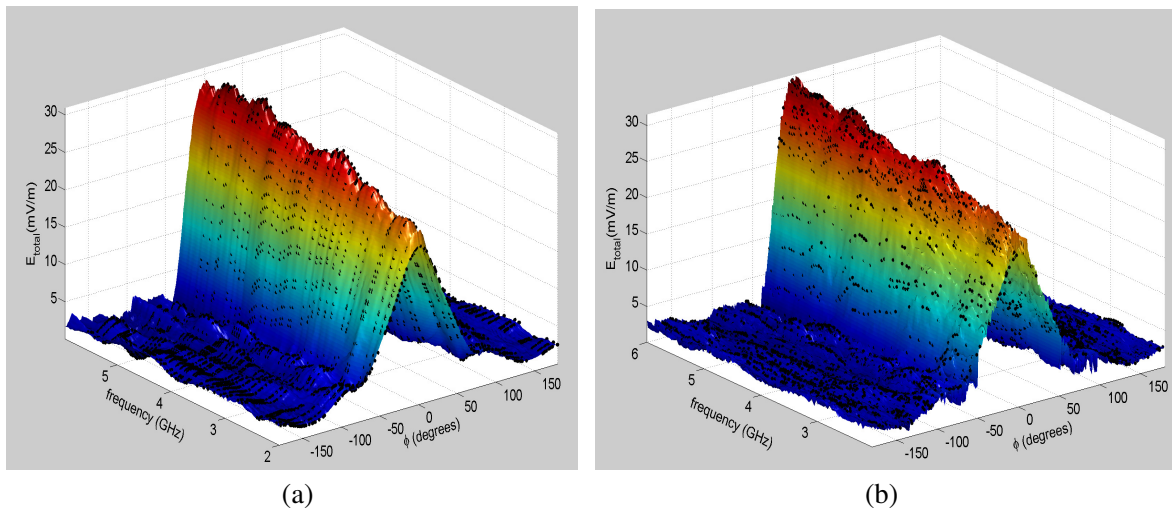

Figure 3. (a) The uniform and (b) non-uniform DCT reconstruction of the dual-ridge horn antenna RFP using 33% of the data points.

In order to determine the number of data points required for reconstruction, the normalized root-mean square error (RMSE) of the frequency dimension reconstruction as compared to the original RFP is calculated as a function of number of data points used. This error analysis is performed for every radiation angle measured, yielding the surface plot shown in Fig. 2(a). Because of the randomness of the data point distribution used, the RMSE of the reconstruction was averaged over 25 trials.

To quantitatively gauge the number of data points needed to reconstruct the RFP, Fig. 2(a) was sliced across the radiation angle ϕ dimension, and the minimum number of data points needed to reconstruct the RFP with a maximum RMSE less that 0.01 (1%) was determined. Fig. 2(b) shows the normalized RMSE of the DCT reconstruction when 33% of the data points is used. The experiment was repeated using the DFT which needed a minimum of 49% of the data points to obtain an RFP reconstruction RMSE of less than 1%. Figs. 3(a) and 3(b) show the DCT uniform and non-uniform reconstructions of the dual-ridge horn RFP using 33% of the data points.

3.2. Bicone Antenna Reconstruction

A center fed, constant voltage, bicone antenna (with length of $12\,\mathrm{cm}$) was modeled from $1\,\mathrm{GHz}$ to $4\,\mathrm{GHz}$ and the E_{total} RFP was created from the calculated total electric field. This antenna model was chosen to test compressive sensing reconstruction on an RFP that varies substantially over the frequency band considered. Fig. 4 shows the RFP of the bicone antenna.
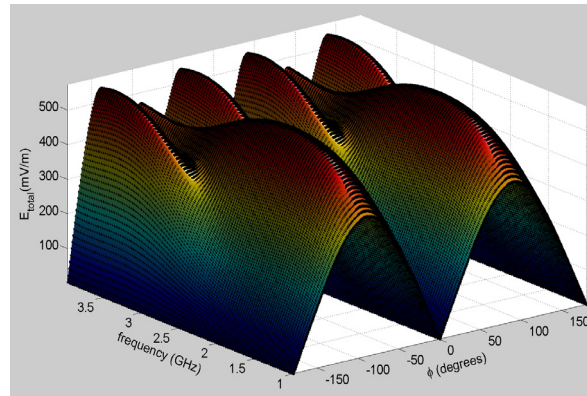

Figure 4. The RFP of a bicone antenna modeled from $1\,\mathrm{GHz}$ to $4\,\mathrm{GHz}$. Superimposed on the RFP are to data points used to create it.
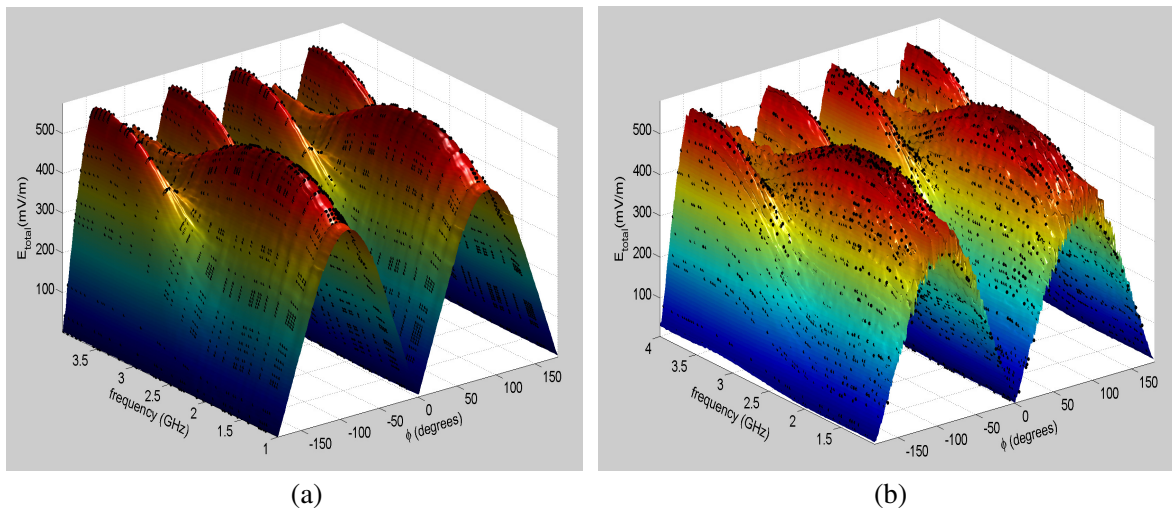

Figure 5. (a) The uniform DCT and (b) non-uniform DCT reconstruction of the bicone antenna RFP using 31% of the data points.
vskip0.02in

To determine the minimum number of data points needed to reconstruct the RFP with an RMSE smaller than 0.01 at every angle, the same procedure as the dual-ridge horn was used. For the bicone antenna, the DCT reconstruction needed 31% of the data points to have an RMSE consistently below 0.01, while the DFT reconstruction needed 65% of the data points. Figs. 5(a) and 5(b) show the uniform and non-uniform DCT reconstructions of the bicone antenna RFPs using 31% of the randomly distributed data points.

3.3. Vivaldi Antenna Reconstruction

Finally, the total electric field RFP of a Vivaldi antenna (with aperture length of $10\,\mathrm{cm}$) was modeled from $4\,\mathrm{GHz}$ to $8\,\mathrm{GHz}$ and its RFP reconstructed using the compressive sensing method. The RFP of the
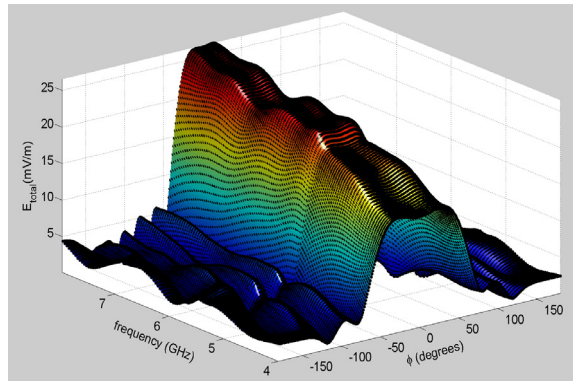
Figure 6. The RFP of a Vivaldi antenna modeled from $4\,\mathrm{GHz}$ to $8\,\mathrm{GHz}$. Superimposed on the RFP are to data points used to create it.
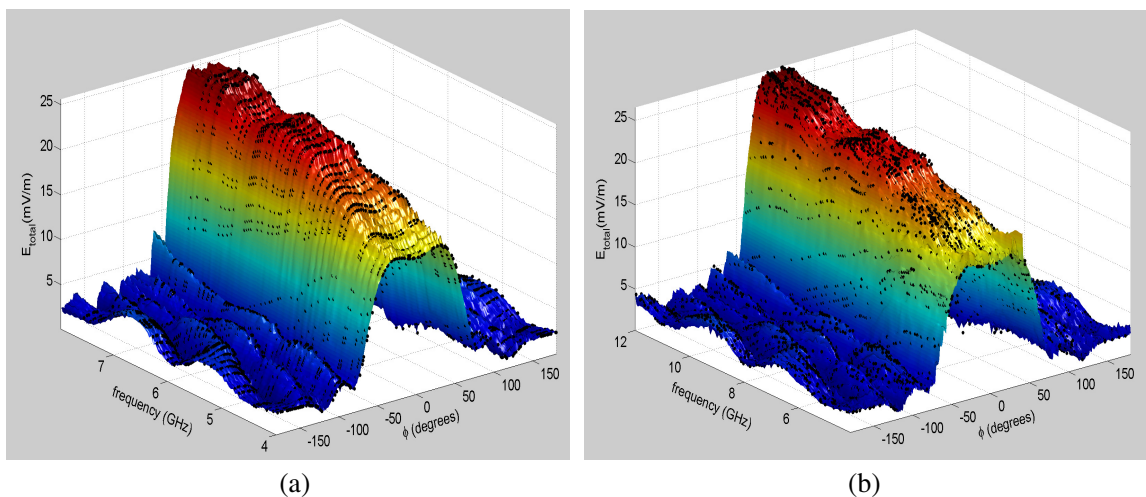

| (a) | (b) |

Figure 7. (a) The uniform DCT and (b) non-uniform DCT reconstruction of the Vivaldi antenna RFP using 33% of the data points.

Vivaldi antenna model is shown in Fig. 6. Using the same procedure as before, the minimum number of points needed to reconstruct the Vivaldi antenna RFP with an RMSE less than 1% was determined to be 33% when using the DCT, and 51% when using the DFT. Figs. 7(a) and 7(b) present the uniform and non-uniform DCT reconstruction of the Vivaldi RFP using 33% of the data points.

4. RFP RECONSTRUCTION IN THE PRESENCE OF NOISE

To explore the effect of noise on RFP reconstruction, the boresight angle traces of the RFPs were reconstructed in the presence of additive white Gaussian noise (AWGN). The ℓ_1-norm minimization constraint, which chooses the reconstruction data that matches the original most closely is replaced with the ℓ_2-norm, which requires the reconstructed signal to be within a small interval ϵ from the original [16]. The ℓ_2-norm minimization,

$$\mathbf{s} \simeq \hat{\mathbf{s}} = \arg\min \|\mathbf{s}'\|_{\ell_2} \quad \text{so that} \quad \|\mathbf{y} - \mathbf{\Phi}\mathbf{s}\|_{\ell_2} \leq \epsilon, \tag{6}$$

is used to reconstruct the RFP traces in varying amounts of AWGN. The l1qc_logbarrier.m routine [13] is used for this purpose.

The RMSE of the boresight trace of the antennas (the broadside trace of the bicone) as a function of the number of data points used for reconstruction are shown in Figs. 8(a) to 8(c). Because of the randomness of the measurements chosen for reconstruction, the RMSEs of the reconstructed RFP were averaged over 100 trials.
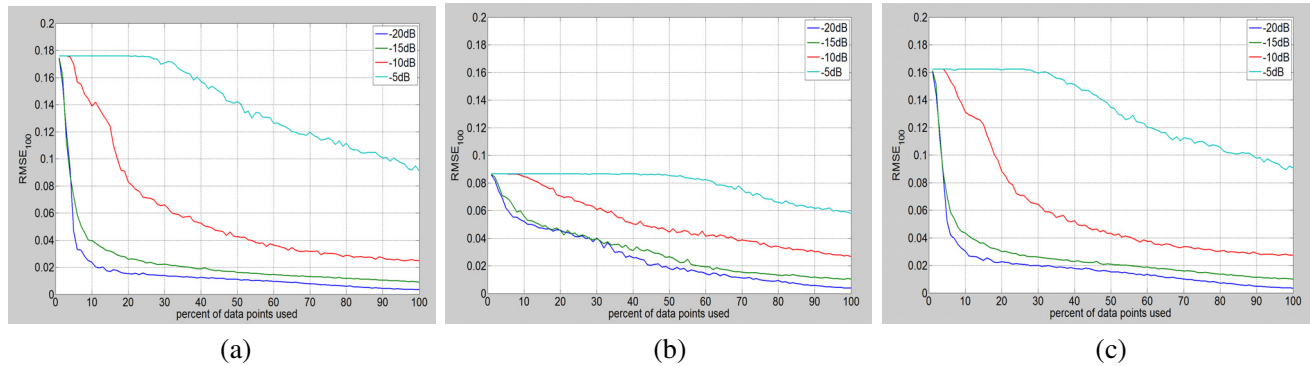
Figure 8. The averaged RMSE of 100 reconstructed (a) dual-ridge horn, (b) bicone, and (c) Vivaldi antenna boresight traces as a function of percentage of data points used.

5. COMPARISON OF THE DFT AND THE DCT IN RADIATION PATTERN RECONSTRUCTION

To analyze the relative efficacy of the uniform versus non-uniform reconstruction, the RMSE of the total normalized uniform and non-uniform RFP reconstructions were compared to the original normalized RFP. The dual-ridge horn was reconstructed with the minimum of 33% of the data points, the bicone with 31% of data points, and the Vivaldi with 33% of data points. Because of the random distribution of the data points chosen for reconstruction, the RMSE of each reconstruction was calculated 100 times and then averaged. The averaged RMSE of the three antenna RFP uniform and non-uniform reconstructions are shown in Table 1. Table 1 shows that the non-uniform methods of antenna RFP reconstruction has a lower RMSE than the uniform reconstruction algorithm with the same number of reconstruction points for all three antennas, and therefore can be considered to be more effective than uniform reconstruction.

Table 1. RMSE(%) of reconstructed RFP.

RMSE	Uniform	Non-uniform
Dual Ridge	0.49	0.36
Bicone	0.91	0.50
Vivaldi	0.70	0.54

vskip-0.04in

6. CONCLUSIONS

Compressive sensing has been demonstrated to reconstruct the RFPs of various modeled wideband antennas. Parallel compressive sensing was used in this study, and the number of data points needed to reconstruct uniform versus non-uniform, DFT versus DCT, RFPs were compared. The effect of AWGN on RFP reconstruction was also studied.

When the RFP reconstructions were analyzed in their angular and frequency dimensions, it was found that the DCT led to convergence with fewer required data points than the DFT for all three antennas. Analysis of the three antenna models considered showed that their RFPs can be reconstructed to within 0.01 of the normalized RMSE with 33% of the original data points.

Computation time was found to be 2.8 seconds to reconstruct the RFPs using 100% of the data (180,000 points) and 0.23 seconds using 33% of the data (59,400 points). The computational platform used was an Intel® Xeon® 2.4 GHz 64-bit computer running MATLAB.

The effect of noise on the compressive sensing reconstruction of antenna RFPs was studied by calculating the RMSE of the antenna boresight trace as a function of data points used in the

reconstruction in varying levels of AWGN. Figs. 8(a) to 8(c) show that the increase in RMSE with increased levels of noise is similar for the three antenna RFPs. These figures show that that the antenna RFPs can be reconstructed to within 1% of their original values with signal to noise ratios of $-15\,\text{dB}$ or smaller (using additional measurement points).

With the possibility of compressive sensing reconstruction of RFPs that uses less measurement data, a new measurement paradigm can be established that will measure the radiation pattern at randomly distributed angles, over randomly distributed frequencies at those angles. In this way, compressive sensing can be used to obtain full wideband antenna radiation characterization with much fewer measurements that are conventionally needed.

REFERENCES

1. Miller, E. K., "Using adaptive estimation to minimize the number of samples needed to develop a radiation or scattering pattern to a specified uncertainty," *ACES Journal*, Vol. 17, No. 3, 176–185, 2002.

2. Werner, D. H. and R. J. Allard, "The simultaneous interpolation of antenna radiation patterns in both the spatial and frequency domains using model-based parameter estimation," *IEEE Transactions on Antennas and Propagation*, Vol. 48, No. 3, 383–392, March 2000.

3. Martí-Canales, J. and L. P. Lighart, "Reconstruction of measured antenna patterns and related time-varying aperture fields," *IEEE Transactions on Antennas and Propagation*, Vol. 52, No. 11, 3143–3147, November 2004.

4. Tkadlec, R. and Z. Nováček, "Radiation pattern reconstruction from the near-field amplitude measurement on two planes using PSO," *Radioengineering*, Vol. 14, No. 4, 63–67, December 2005.

5. Rammal, R., M. Lalande, M. Jouvet, N. Feix, J. Andrieu, and B. Jecko, "Far-field reconstruction from transient near-field measurements using cylindrical modal development," *International Journal of Antennas and Propagation*, Article ID 798473, 2009.

6. Koh, J., A. De, T. K. Sarkar, H. Moon, W. Zhao, and M. Salazar-Palma, "Free space radiation pattern reconstruction from non-anechoic measurements using an impulse response of the environment," *IEEE Transactions on Antennas and Propagation*, Vol. 60, No. 2, 821–831, February 2012.

7. Wei, S.-J., X.-L. Zhang, J. Shi, and K.-F. Liao, "Sparse array microwave 3-D imaging: Compressed sensing recovery and experimental study," *Progress In Electromagnetic Research*, Vol. 135, 161–181, 2013.

8. Verdin, B. and P. Debroux, "2D and 3D far-field radiation patterns reconstruction based on compressive sensing," *Progress In Electromagnetic Research M*, Vol. 46, 47–56, 2016.

9. Baraniuk, R. G., "Compressive sensing," *IEEE Signal Processing Magazine*, 118, July 2007.

10. Fornasier, M. and H. Rauhut, *Handbook of Mathematical Methods in Imaging*, Chapter 6, 187–228, Springer, 2011.

11. Fornasier, M. and H. Rauhut, *Handbook of Mathematical Methods in Imaging*, Vol. 1, Springer, 2010.

12. Candés, E., J. Romberg, and T. Tao, "Robust uncertainty principles: Exact signal reconstruction from highly incomplete frequency information," *IEEE Transactions on Information Theory*, Vol. 52, No. 2, 489–509, February 2006.

13. Romberg, J., L1qc_logbarrier.m.statweb.stanford.edu/čandes/l1magic/, October 2005, accessed: 2016-11-15.

14. ANSYS, *HFSS for Antenna Design Training Manual*, 1st Edition, ANSYS, May 2016.

15. Fang, H., S. A. Vorobyov, H. Jiang, and O. Taheri, "Permutation meets parallel compressed sensing: How to relax restricted isometry property for 2D sparse signals," *IEEE Transactions on Signal Processing*, Vol. 62, No. 1, 196–210, January 2014.

16. Boufonos, P., M. F. Duarte, and R. G. Baraniuk, "Sparse signal reconstruction from noisy compressive measurement using cross validation," *2007 IEEE/SP 14th Workshop on Statistical Signal Processing, IEEE Signal Processing Society*, IEEE, August 2007.